Available online at www.sciencedirect.com
ScienceDirect
Advances in Space Research 41 (2008) 259–266
ADVANCES IN SPACE RESEARCH (a COSPAR publication)
www.elsevier.com/locate/asr

Evolution of solar wind structures from 0.72 to 1 AU

L. Jian [a,*], C.T. Russell [b], J.G. Luhmann [c], R.M. Skoug [d]

[a] Institute of Geophysics and Planetary Physics, University of California, Los Angeles, 595 Charles E. Young Drive East, 6862 Slichter, Los Angeles, CA 90095, USA
[b] Institute of Geophysics and Planetary Physics, University of California, Los Angeles, 595 Charles E. Young Drive East, 6869 Slichter, Los Angeles, CA 90095, USA
[c] Space Sciences Laboratory, University of California, Berkeley, CA 94720, USA
[d] Space Science and Applications, Los Alamos National Laboratory, Los Alamos, NM 87545, USA

Received 20 November 2006; received in revised form 20 February 2007; accepted 12 March 2007

Abstract

Understanding the evolution of solar wind structures in the inner heliosphere as they approach the Earth is important to space weather prediction. From the in situ solar wind plasma and magnetic field measurements of Pioneer Venus Orbiter (PVO) at 0.72 AU (1979–1988), and of Wind/Advanced Composition Explorer (ACE) missions at 1 AU (1995–2004), we identify and characterize two major solar wind structures, stream interaction regions (SIRs) and interplanetary coronal mass ejections (ICMEs). The average percentage of SIRs occurring with shocks increases significantly from 3% to 24% as they evolve from 0.72 to 1 AU. The average occurrence rate, radial extent, and bulk velocity variation of SIRs do not change from 0.72 to 1 AU, while peak pressure and magnetic field strength both decrease with the radial evolution of SIRs. Within the 0.28 AU distance from the orbit of Venus to that of Earth, the average fraction of ICMEs with shocks increases from 49% to 66%, and the typical radial extent of ICMEs expands by about a fraction of 1.4, with peak pressure and magnetic field strength decreasing significantly. The mean occurrence rate and expansion velocity of ICMEs do not change from 0.72 to 1 AU.

Keywords: Interplanetary coronal mass ejection or ICME; Stream interaction; Radial evolution; Pioneer Venus Orbiter or PVO

1. Introduction

There are two major types of solar wind disturbances. One is the quasi-steady stream interaction region (SIR) where a fast stream overtakes a leading slow stream and outruns a following slow stream (e.g., reviewed by Balogh et al., 1999a). The other one is the transient, interplanetary coronal mass ejection (ICME) (e.g., reviewed by Crooker et al., 1997). They both can be associated with energetic particles and affect geomagnetic activities. Their evolution has been an outstanding problem since early solar wind observations, because there are few simultaneous observations of the solar wind in the inner solar system.

Stream interactions occur throughout the solar cycle, as velocity differentials at the coronal sources remain a feature of the solar wind at all times (Balogh et al., 1999b). If the flow pattern from the Sun is roughly time-stationary, then the SIRs form spirals corotating with the Sun in the solar equatorial plane, named corotating interaction regions (CIRs) (Smith and Wolfe, 1976; Gosling and Pizzo, 1999). But corotating patterns rarely last more than one solar rotation near solar maximum, as the coronal sources change significantly on the time scale of a solar rotation (Balogh et al., 1999b). In this study we have made surveys of SIRs, including not only the traditionally considered CIRs (specified in the surveys), but also transient and non-recurrent stream

* Corresponding author.
E-mail addresses: jlan@igpp.ucla.edu (L. Jian), ctrussel@igpp.ucla.edu (C.T. Russell), jgluhman@ssl.berkeley.edu (J.G. Luhmann), rskoug@lanl.gov (R.M. Skoug).

0273-1177/$30 © 2007 COSPAR. Published by Elsevier Ltd. All rights reserved.
doi:10.1016/j.asr.2007.03.023

interactions which also can affect geomagnetic activity (Jian et al., 2006a).

Forsyth and Marsch (1999) using Helios data found that not all SIRs between 0.3 and 1 AU contain a sharp stream interface (SI). A greater number of clearly discontinuous interfaces are observed at 1 AU than 0.3 AU (Gosling et al., 1978; Schwenn, 1990), suggesting that the steepening of the interface boundary takes place between these distances due to the increasing compression of the fast stream against slow stream (Forsyth and Marsch, 1999). In addition, Balogh et al. (1999b) interpreted the absence of a clear SI in the majority of CIRs observed close to the Sun for several reasons, one of which was that the transitions between slow and fast streams in the corona could be quite complex and temporal variable (Schwenn, 1990) and the SIs do not always need to have the same profile or steepness.

The above studies of the properties and dynamics of the solar wind in the range 0.3–1 AU are based on the two Helios spacecraft (e.g., Richter and Luttrell, 1986; Schwenn, 1990; Schwenn and Marsch, 1990), which orbited the Sun from 0.3 and 1 AU from 1975 to 1981. Because its orbit was very eccentric, Helios spent most of its life at aphelion near 1 AU with just occasional excursions to 0.3 AU. Thus there is not good statistical coverage close to the Sun, nor is there complete solar cycle coverage. The changing radial distance also affects the identification of the recurrence of SIRs. Hence, other datasets such as the one of the long-lived Pioneer Venus Orbiter (PVO) data at 0.72 AU can provide a much needed supplement to the Helios data. While farther out in the heliosphere, Gosling et al. (1993, 1995a), Burlaga et al. (1997) and other investigators have studied CIRs extensively using Ulysses and Voyager data, we need to understand for space weather purpose how CIRs evolve before they reach 1 AU.

ICMEs undergo significant changes as they evolve from the Sun. Recent work on the multiple spacecraft (Gosling et al., 1995b; McAllister et al., 1996; Reisenfeld et al., 2003; Riley et al., 2003) has compared the ICME observations at 1 AU and at Ulysses, which is up to ~5 AU. Using α particle enhancements, Paularena et al. (2001) and Richardson et al. (2002) traced CMEs along the Sun–Earth–Ulysses–Voyager 2, as far as 58 AU. Such events observed by multiple well-separated spacecraft are important for understanding ICME evolution, but the observations are very rare and they do not necessarily represent the typical evolution of ICMEs as well as the solar cycle variability. As with CIRs, it is most important for space weather predictions to understand ICME evolution within 1 AU.

A variety of different approaches have been used to identify ICMEs. Wang and Richardson (2004) and Wang et al. (2005) took abnormally low proton temperature as the primary criteria to identify "probable" ICMEs, and Liu et al. (2005) used enhanced α abundances and depressed proton temperatures to identify ICMEs. There are many features to identify ICMEs (e.g., Neugebauer and Goldstein, 1997; Cane and Richardson, 2003; Russell and Shinde, 2005). Many of these signatures appearing not to be unique to ICMEs or by themselves sufficient conditions to identify ICMEs (e.g., Gosling, 1997; Neugebauer and Goldstein, 1997). Low proton temperature can also be associated with slow streams, and appear close to sector boundaries. Because we wish to compare quantitatively the results at different heliocentric radii, it is important to use as similar criteria as possible at different distances.

We have already completed a study at 1 AU (Jian et al., 2006a,b). Herein, we focus on the inner heliosphere at 0.72 AU, and compare these results to our 1 AU study. These results are important for accurate space weather predictions at the Earth. In future studies, we plan to extend our study to other distances, using Ulysses data.

2. Data set

The surveys of SIRs and ICMEs at 0.72 AU are based on the observations by Pioneer Venus Orbiter (PVO) (Colin, 1980; Colin and Hunten, 1977) during January 1979 to August 1988. The plasma analyzer (Intriligator et al., 1980) and magnetometer (Russell et al., 1980) provided the interplanetary solar wind measurements. For our purpose, we use the averaged 10-min-resolution plasma data and 0.5-s-resolution magnetometer data (with measurements down stream of Venus bow shock removed), in the Venus solar orbital (VSO) system. Considering the large data gaps, we use the observed event number divided by the fraction of usable data each year, to estimate the annual number of events. The resolution of magnetometer data is high enough to identify shocks, but the low-resolution plasma data by itself would have left several ambiguous identifications.

Our comparison study at 1 AU uses observations by the Wind (1995–2004) spacecraft and Advanced Composition Explorer (ACE) (1998–2004). We use the 93-s-resolution SWE (Ogilvie et al., 1995) and MFI (Lepping et al., 1995) from Wind, in addition to the 64-s-resolution validated Level 2 data of SWEPAM (McComas et al., 1998) and MAG (Smith et al., 1998) on ACE. The data are in geocentric solar magnetospheric (GSM) coordinates. To identify shocks, higher-resolution Wind 3DP (Lin et al., 1995) and MFI data are examined. Although VSO and GSM coordinates are different, it does not affect our following statistical study, in which only scalar measurements are examined.

3. Criteria of SIRs and ICMEs

To assist us in classifying ICMEs and SIRs, and in quantifying the interaction strength (Jian et al., 2006a,b), we use the temporal behavior of a physically based and empirically useful compound parameter, total perpendicular pressure (P_t) (Russell et al., 2005), the sum of the magnetic pressure and plasma (including proton, electron, and α) pressure perpendicular to the magnetic field. In addition, since energetic particle data are not always available for disturbance identification, the P_t calculated from the more usually available plasma and magnetic field measurements gives much more complete coverage of the solar cycle, as well as a uniform criterion across the solar cycle and at the two radial distances.

Following our study of SIRs at 1 AU (Jian et al., 2006a), the required criteria of SIRs are: an increase of solar wind speed (V_p), a peak of P_t with gradual declines at two sides, a compression of proton number density (N_p) and magnetic field (**B**), an enhancement of proton temperature (T_p), and the flow deflection (1 AU data available, and 0.72 AU data unavailable). The stream interface is defined to be at the peak of P_t, where usually V_p and T_p increase and N_p begins to drop after a N_p compression region. The forward/reverse shocks are classified from the expected signatures of plasma and magnetic field (Jian et al., 2006a,b). To discriminate between shocks and shock-like structures, the simultaneous variation of N_p, T_p, **B**, and other parameters are required; we also rotated the magnetic field data into shock normal coordinates and checked for the existence of the expected shock associated waves and changes in the field consisted with the Rankine–Hugoniot relationships.

Fig. 1 illustrates two SIRs without shocks, respectively, observed at 0.72 and 1 AU. Besides the above SI signatures, the entropy [defined as $\ln(T_p^{3/2}/N_p)$] increases at the SI, marked as dashed line b. The transition from slow stream to fast stream is gradual at 0.72 AU, taking ~6.5 h, while the transition at 1 AU is much sharper, taking only ~15 min.

As in our study of ICMEs at 1 AU (Jian et al., 2006b), the ICMEs are identified from a combination of the P_t enhancement, a stronger than ambient magnetic field, a relatively quiet and smooth rotation in **B** (Gosling, 1990, and references therein), a decline of V_p, low T_p, an α abundance enhancement, and bidirectional solar wind electron strahls (if these data available). However, none of the above characteristics is a necessary criterion when some other features of plasma and magnetic field are prominent. In general, we require the presence of at least three features for ICMEs,

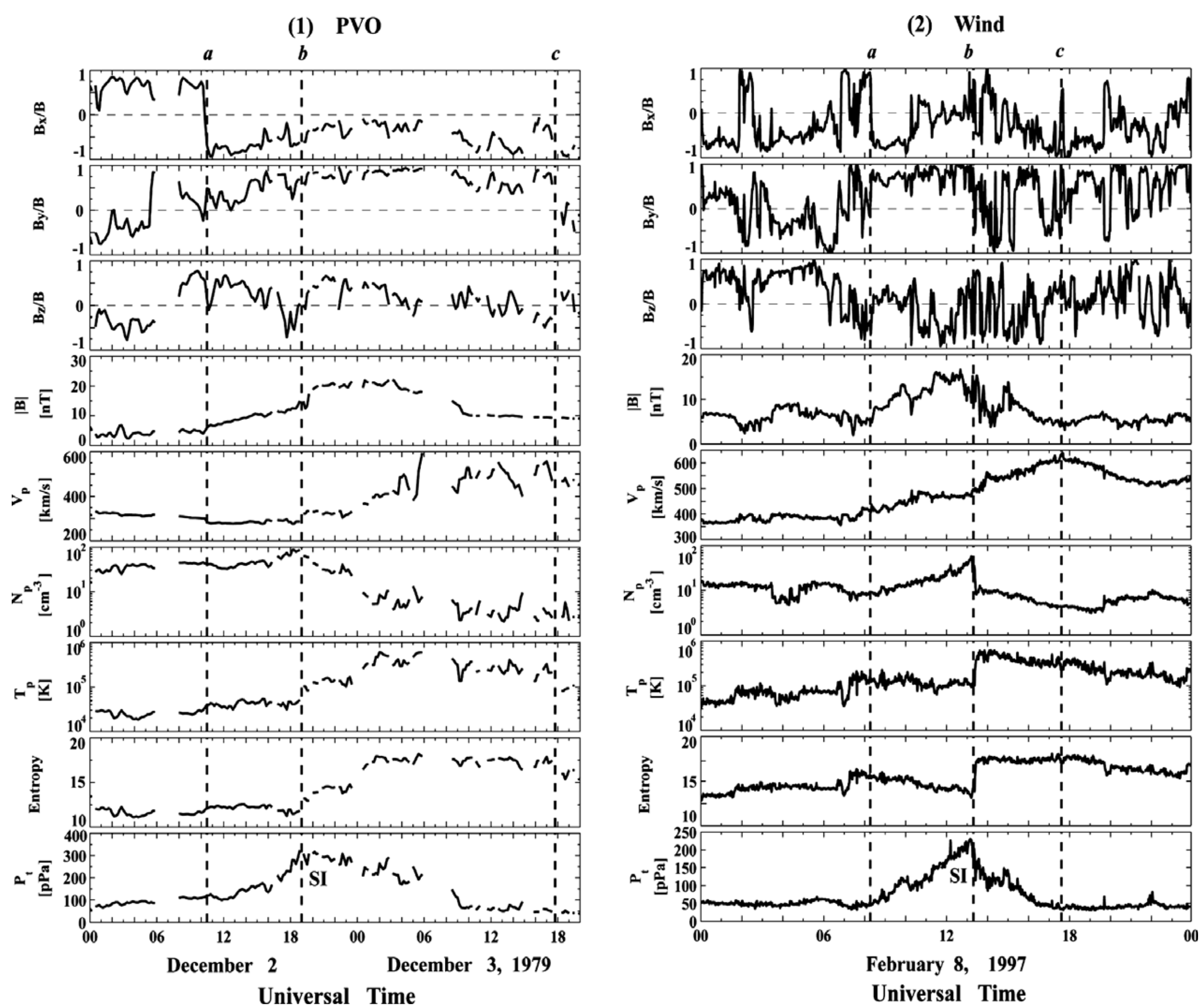

Fig. 1. SIR events without shocks, from PVO and Wind data. From top to bottom: direction cosines of magnetic field in VSO or GSM coordinates, magnetic field strength, solar wind speed, proton density, proton temperature, entropy [defined as $\ln(T_p^{3/2}/N_p)$], and total perpendicular pressure. Dashed lines a and c indicate the boundaries of the SIR; dashed line b marks the stream interface (SI).

rather than separately identify magnetic clouds (MCs) and non-cloud ICMEs. In all, 82% of our ICMEs at 1 AU overlap in Cane and Richardson (2003) list, but some have different boundaries.

Often the magnetic clouds are treated as a specific subset of ICMEs. They are characterized by a low β and large coherent internal magnetic field rotations through a relatively large angle (e.g., Burlaga et al., 1981; Klein and Burlaga, 1982). We find that the P_t temporal profiles can be sorted into three characteristic patterns, which are correlated with the observed MC signatures (Jian et al., 2006b). Depending on the P_t temporal profiles, we define three groups of ICMEs. Corresponding to the Group 1, 2, and 3 ICMEs, the P_t profile following the shock and/or sheath increases, respectively, has a central pressure maximum, or a steady plateau, or a gradual decay. This pattern is consistent with each ICME having a causative central flux rope, with the three groups of P_t profiles being due to different distances of approach to the central flux rope. So MCs are usually classified as Group 1 events, where the spacecraft penetrated the center of flux rope. About 89% of our Group 1 events at 1 AU are considered as MC = 2 and 1 events by Cane and Richardson (2003).

Fig. 2 shows two Group 1 ICMEs at 0.72 and 1 AU, where we can see classic flux rope structures, and they are MCs. There are more disturbances in the magnetosheath region between the dashed lines a and b, at 1 AU than 0.72 AU, and the ICME at 1 AU lasted about twice as long as that at 0.72 AU. We use the term magnetosheath for the region between the shock and the obstacle because it differs in no substantial way from the magnetosheath observed at planets, e.g., Liu et al. (2006) shows mirror mode structures ahead of ICMEs, analogous to planetary magnetosheaths. To be consistent across the three groups of ICMEs and also due to the geoeffectiveness of the magnetosheath region, we define our ICME boundaries to include the magnetosheath region (if there is one).

Besides the SIRs and ICMEs, we have also identified hybrid events, which are composed of an SIR and an ICME or of more than one ICME. If the structures of these

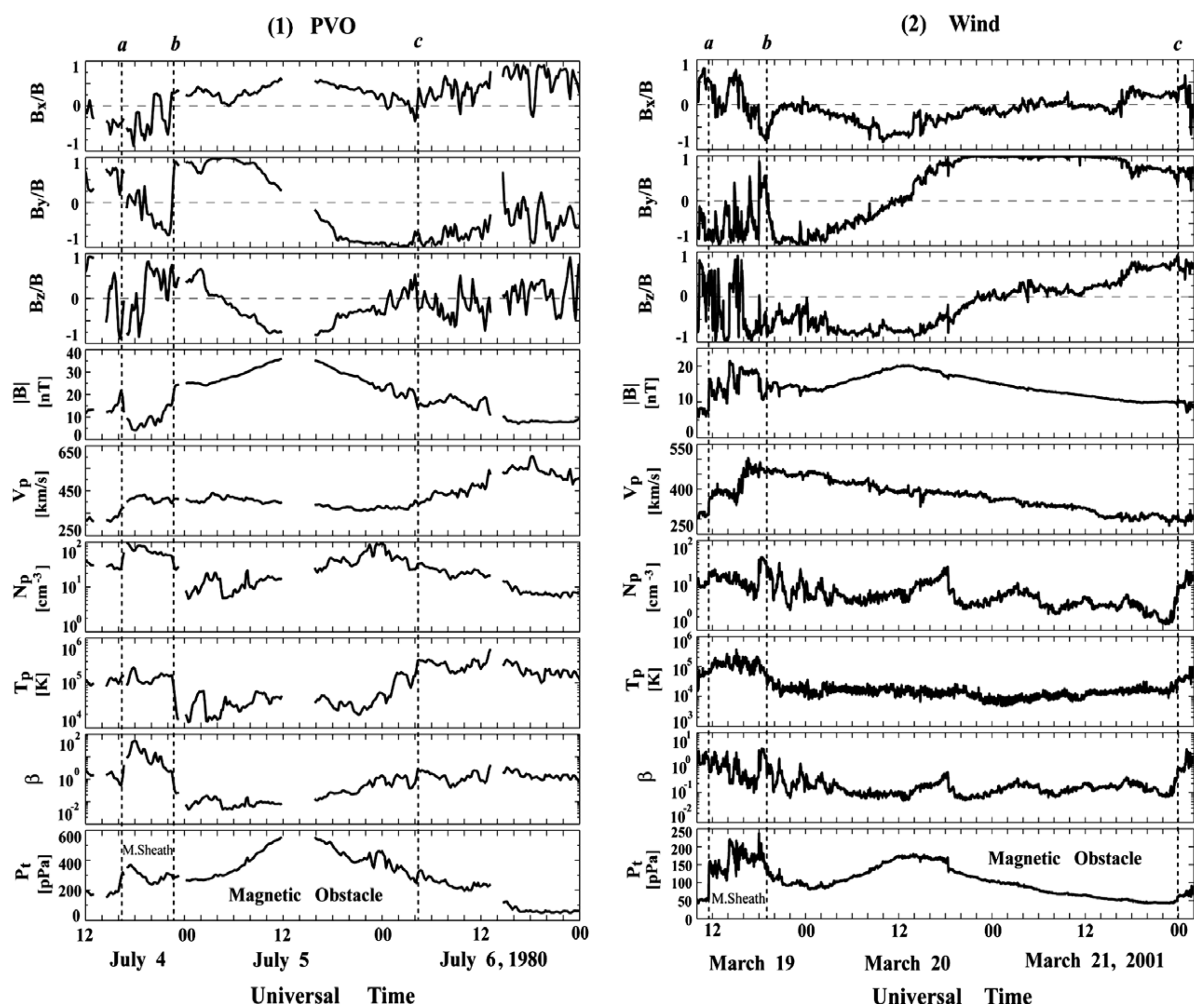

Fig. 2. Two Group 1 ICMEs from PVO and Wind observations. From top to bottom: direction cosines of magnetic field in VSO or GSM coordinates, magnetic field strength, bulk velocity, proton density, proton temperature, β (the ratio of plasma thermal pressure to magnetic pressure), and total perpendicular pressure. M. Sheath: magnetosheath, the interval between the dashed lines a and b; magnetic obstacle: the region between dash lines b and c.

SIRs or ICMEs are still representative, we include them into SIRs or ICMEs list as appropriate. The specific and thorough examination of the V_p, T_p, **B** profiles, and other features, leaves few ambiguous identifications.

4. Comparison of SIRs properties at 0.72 and 1 AU

Table 1 compares the properties of SIRs (including CIRs) at 0.72 and 1 AU. At 0.72 AU, from 1979 to 1988, there are 203 SIRs, including 99 CIRs. Using the estimation method in Section 2, normalizing to full years of observation, we find 342 SIRs and 163 CIRs. Comparing to the observed 365 SIRs (196 CIRs) at 1 AU, the average annual occurrence rates of SIRs and CIRs do not change much from 0.72 to 1 AU, and the CIR fraction among SIRs only increases slightly from 49% to 54%.

From 0.72 to 1 AU, the shock association rate increases greatly, from 3.4% to 24.1%. At 0.72 AU, we only find seven shocks associated with SIRs, five of which are forward shocks. The preponderance of forward shocks agrees with our results at 1 AU (Jian et al., 2006a). At the two distances, near the ecliptic plane, about 70% of shocks occurring with SIRs are forward shocks. We estimate radial extent (W) as the product of duration and the average of V_{max} and V_{min} of one event. The average radial extents of SIRs and CIRs stay around 0.4 AU from 0.72 to 1 AU, and either at 0.72 or 1 AU, CIRs are typically larger than SIRs.

Table 1 lists the comparison through the average and median values of each property of SIRs and CIRs. As SIRs evolve from 0.72 to 1 AU, the median peak pressure (P_{max}) of SIRs decreases from 410 to 143 pPa, and the maximum magnetic field strength (B_{max}) decreases by about 5 or 6 nT. The average velocity change (ΔV) over the SIRs nearly has no significant change from 0.72 to 1 AU, while the ΔV of CIRs increases about 20 km/s within the 0.28 AU separation. From 0.72 to 1 AU, for both SIRs and CIRs, the ratio of the duration of leading part before the stream interface over the duration of trailing part after the interface ($R_D = D_{before}/D_{after}$), varies a little.

In addition, the fraction of SIRs with sharp interfaces is higher at 1 AU than at 0.72 AU, in agreement with Balogh et al. (1999b), who found the compression between the streams becomes increasingly effective in shaping the profile of the solar wind parameters as beyond 0.5 AU, probably due to the gradually increasing inclination of the Parker spiral with respect to the radial direction. It may be also related to the turbulence along the interface.

Table 1
Comparison of SIRs properties at 0.72 and 1 AU

Quantity	0.72 AU	1 AU
SIR no. (per year)	20.3 (34.2)*	36.5
CIR no. (per year)	9.9 (16.3)	19.6
CIR fraction (%)	48.8	53.7
SIR shock association rate (%)	3.4	24.1
CIR shock association rate (%)	3.0	31.0
Average of SIR properties		
Radial extent (AU)	0.40 ± 0.02	0.41 ± 0.01
P_{max} (pPa)	458 ± 14	176 ± 6
B_{max} (nT)	21.8 ± 0.4	15.5 ± 0.3
ΔV (km/s)	224 ± 6	230 ± 5
R_D (D_{before}/D_{after})	1.06 ± 0.05	1.21 ± 0.07
Median of SIR properties		
Radial extent (AU)	0.34	0.37
P_{max} (pPa)	410	143
B_{max} (nT)	20.5	14.5
ΔV (km/s)	215	210
R_D (D_{before}/D_{after})	0.85	0.8
Average of CIR properties		
Radial extent (AU)	0.46 ± 0.02	0.44 ± 0.02
P_{max} (pPa)	473 ± 18	214 ± 9
B_{max} (nT)	22.1 ± 0.5	17.2 ± 0.4
ΔV (km/s)	257 ± 9	285 ± 6
R_D (D_{before}/D_{after})	1.10 ± 0.08	1.42 ± 0.12
Median of CIR properties		
Radial extent (AU)	0.42	0.40
P_{max} (pPa)	440	180
B_{max} (nT)	22.0	16.3
ΔV (km/s)	258	270
R_D (D_{before}/D_{after})	0.94	0.87

* The value in paranthesis is estimated event number, considering data gaps.

5. Comparison of ICMEs properties at 0.72 and 1 AU

From PVO data (1979–1988), we have identified 124 ICMEs in all, equivalent to the occurrence of 203 ICMEs accounting for missing data. The occurrence rate has strong solar cycle dependence, from 4 or 5 events per year near solar minimum up to 18 near solar maximum. Due to many data gaps, only 97 ICMEs have pressure features clear enough to be classified into one of the three groups.

As listed in Table 2, Group 1, 2, and 3 ICMEs, respectively, have fractional occurrence rates of 34%, 26%, and

Table 2
Comparison of ICMEs properties at 0.72 and 1 AU

Quantity	0.72 AU	1 AU
No. (per year)	12.4 (20.3)	23.0
ICME shock association rate (%)	49	66
Fractions among classifiable ICMEs (%)		
Group 1	34	36
Group 2	26	25
Group 3	40	39
Average over all ICMEs		
Radial extent (AU)	0.28 ± 0.01	0.41 ± 0.01
P_{max} (pPa)	704 ± 48	252 ± 19
B_{max} (nT)	31.1 ± 1.4	19.3 ± 0.7
V_{mean} (km/s)	476 ± 12	493 ± 8
$\|\Delta V\|$ (km/s)	132 ± 7	139 ± 6
Median of all ICMEs		
Radial extent (AU)	0.27	0.37
P_{max} (pPa)	560	150
B_{max} (nT)	26	16
V_{mean} (km/s)	457.5	462.5
$\|\Delta V\|$ (km/s)	115	110

40% at 0.72 AU. These are similar to the ratios at 1 AU (Jian et al., 2006b). This similarity suggests that the inner core and the magnetosheath of the ICMEs expand at the same rate as the ICMEs move outward from the Venus orbit to Earth orbit.

From 0.72 to 1 AU, the average shock association rate increases from 49% to 66%. And at the two distances, the shock association rate and radial extent roughly increase with solar activity. As the ICME expands in its journey from 0.72 to 1 AU, the median radial extent increases by a factor of 1.38, from 0.27 to 0.37 AU. So the radial extent W varies as $W = 0.37 \times R^{0.95}$ (AU), where R is the heliocentric distance in AU. We note that if the ICME remains anchored to the Sun as it expands and if the magnetic flux and helicity are constant, we expect that the radial extent of the flux rope to vary as R. Based on MCs between 0.3 and 4.2 AU, Bothmer and Schwenn (1994) obtained a radial width of MCs $W = 0.24 \times R^{0.78\pm0.10}$; a theoretical calculation by Chen (1996) yielded $W \sim R^{0.88}$ for flux rope between 0.3 and 5 AU. Our conclusion is consistent with these two studies, except that our W includes the magnetosheath region (if there is one).

From 0.72 to 1.0 AU, the average of the maximum interaction strength, P_{max}, decreases from 704 ± 48 to 252 ± 19 pPa, more greatly than SIRs; and the median of P_{max} decreases from 560 to 150 pPa, as shown in Table 2. The median value of B_{max} decreases from 26 to 16 nT, as expected. The median value of mean velocity (V_{mean}), estimated as the average of the V_{max} and V_{min} over ICMEs, has no obvious change from 457.5 to 462.5 km/s.

We define the expansion velocity as the speed difference between the forward and trailing edges of ICMEs, i.e., the absolute value of velocity change ($|\Delta V|$) over an ICME. If the expansion is due to excess pressure inside the ICME, we might expect the rate of expansion to decrease as the ICME moved outward and the pressure dropped. Contrary to our expectation, from 0.72 to 1 AU, the expansion velocity does not change significantly. The median of $|\Delta V|$ is 115 km/s at 0.72 AU, and 110 km/s at 1 AU.

Given a sound speed of the background solar wind as 60 km/s and an Alfvén speed as 40 km/s (Kivelson and Russell, 1995), the fast magnetosonic speed (V_{MS}) is about 72 km/s at 1 AU. We know the solar wind number density and the radial component of the magnetic field both vary inversely as the square of heliocentric distance, while the tangential component of the magnetic field varies inversely as the first power. Assuming the ion temperature decrease as the inverse of the distance, and the electron temperature varies inversely as the square root of the heliocentric radius, the fast V_{MS} is about 79 km/s at 0.72 AU. So the average ICME expansion velocity of ~110 km/s is larger than the fast V_{MS} of ambient solar wind at both heliocentric distances, indicating the ICMEs are super-magnetosonically expanding from 0.72 to 1 AU. This conclusion differs slightly from that of earlier researchers who concluded that the expansion speed of ICMEs is of the order of the Alfvén speed in the solar wind (Klein and Burlaga, 1982; Wang et al., 2005), but is consistent with the common occurrence of shocks at the leading edges of ICMEs at both 0.72 and 1 AU.

6. Concluding remarks

The stream interaction depends on heliocentric distance as a function of the Parker spiral angle. In the range 0.72 to 1 AU examined in this study, we find a steeper transition with increased heliocentric distance, in agreement with the greater number of clearly discontinuous interfaces observed at 1 AU than 0.3 AU by Gosling et al. (1978) and Schwenn (1990).

The occurrence rates of SIRs, CIRs, and ICMEs do not change much from the Venus to the Earth orbit, while their shock association rates both increase significantly. The fractional occurrence of the three groups of ICMEs changes little from 0.72 to 1 AU. The scale size and ΔV of either SIRs or CIRs do not change significantly within the 0.28 AU separation, while P_{max} and B_{max} both decrease. The median value of P_{max} of SIRs decreases by a factor of 2.87, from 410 to 143 pPa. ICMEs expand almost super-magnetosonically from 0.72 to 1 AU, with the median radial extent increasing by a factor of 1.38, and median P_{max} decreasing by a factor of 3.73, from 560 to 150 pPa. The median expansion velocity of ICMEs stays around 110 km/s over the range 0.72–1.0 AU.

From 0.72 to 1 AU, the background solar wind pressure decreases from ~93 to 45 pPa. So, with the increase of heliocentric distance, the size of the P_{max} decrease of ICMEs is larger than that of SIRs, and both of them are larger than that of the background solar wind. The magnetic field strength of background solar wind decreases from 11.2 to 7.0 nT, by ~1.6 times. The scale of the decrease of B_{max} of ICMEs (26.0–16.0, 1.6 times) is bigger than that of the background solar wind, while the latter is slightly larger than that of SIRs (20.5–14.5, 1.4 times).

We note that the observations at the two distances are in different solar cycles, separated by one 22-year Hale cycle. We have found no literature pertinent to the variation of ICMEs and SIRs properties from solar cycle to solar cycle. However, if there is variation of the properties with solar cycle the statistical comparison could be affected. Eventually we hope to compare data at different distances obtained simultaneously. The ACE, Wind and STEREO data, with the on-going Venus Express (Titov et al., 2006) and the proposed NASA's LWS Sentinels mission and ESA's Solar Orbiter mission (Marsch et al., 2005) would provide a good opportunity to make simultaneous measurements at different heliocentric distances.

Acknowledgements

This work has been jointly supported by the IGPP branch at Los Alamos National Lab (LANL) and by the National Aeronautics and Space Administration's STEREO program through a grant administered by UCB. We thank the MIT and Goddard plasma team (A.J. Lazarus and K.W. Ogilvie), 3DP plasma team (R.P. Lin), the magnetometer team (R.P. Lepping) and CDAWeb for making Wind data publicly available. We are grateful to the PIs of the plasma analyzer (D.J. McComas) and the magnetometer (C.W. Smith) for making ACE data available. Work at Los Alamos was performed under the auspices of the US Department of Energy, with financial support from the NASA ACE program.

References

Balogh, A., Gosling, J.T., Jokipii, J.R., Kallenbach, R., Kunow, H. (Eds.), Corotating Interaction Regions, Proceedings of an ISSI Workshop, Space Sci. Rev., vol. 89, Dordrecht, the Netherlands, 1999.

Balogh, A., Bothmer, V., Crooker, N.U., et al. The solar origin of corotating interaction regions and their formation in the inner heliosphere. Space Sci. Rev. 89, 141–178, 1999b.

Bothmer, V., Schwenn, R. Eruptive prominences as sources of magnetic clouds in the solar wind. Space Sci. Rev. 70, 215, 1994.

Burlaga, L.F., Ness, N.F., Belcher, J.W. Radial evolution of corotating merged interaction regions and flows between ~14 AU and ~43 AU. J. Geophys. Res. 102, 4661, 1997.

Burlaga, L.F., Sittler, E., Mariani, F., Schwenn, R. Magnetic loop behind an interplanetary shock: Voyager, Helios and IMP-8 observations. J. Geophys. Res. 86, 6673, 1981.

Cane, H.V., Richardson, I.G. Interplanetary coronal mass ejections in the near-Earth solar wind during 1996–2002. J. Geophys. Res. 108 (A4), 1156, 2003.

Chen, J. Theory of prominence eruption and propagation: interplanetary consequences. J. Geophys. Res. 108 (A4), 1156, 1996.

Colin, L. The Pioneer Venus program. J. Geophys. Res. 85, 7575–7598, 1980.

Colin, L., Hunten, D.M. Pioneer Venus experiment descriptions. Space Sci. Rev. 20, 451, 1977.

Crooker, N., Joselyn, J.A., Feynman, J. (Eds.), Coronal Mass Ejections, Geophys. Monogr. Ser., vol. 99, AGU, Washington, DC, 1997.

Forsyth, R.J., Marsch, E. Solar origin and interplanetary evolution of stream interface. Space Sci. Rev. 89, 7–20, 1999.

Gosling, J.T. Coronal mass ejections: an overview, in: Crooker, N., Joselyn, J.A., Feynman, J. (Eds.), Coronal Mass Ejections, Geophys. Monogr. Ser., vol. 99, AGU, Washington, DC, p. 9, 1997.

Gosling, J.T. Coronal mass ejections and magnetic flux ropes in interplanetary space, in: Russell, C.T., Priest, E.R., Lee, L.C. (Eds.), Physics of Magnetic Flux Ropes, Geophys. Monogr. Ser., vol. 58, AGU, Washington, DC, p. 343, 1990.

Gosling, J.T., Pizzo, V.J. Formation and evolution of corotating interaction regions and their three dimensional structure. Space Sci. Rev. 89, 21–52, 1999.

Gosling, J.T., Asbridge, J.R., Bame, S.J., Feldman, W.C. Solar wind stream interfaces. J. Geophys. Res. 82, 1401–1412, 1978.

Gosling, J.T., Bame, S.J., McComas, D.J., et al. Latitudinal variation of solar wind corotating stream interaction regions: Ulysses. Geophys. Res. Lett. 20, 2789, 1993.

Gosling, J.T., Bame, S.J., McComas, D.J., et al. Solar wind corotating interaction regions out of the ecliptic plane: Ulysses. Space Sci. Rev. 72, 99, 1995a.

Gosling, J.T., McComas, D.J., Phillips, J.L., et al. A CME-driven solar wind disturbance observed at both low and high heliographic latitudes. Geophys. Res. Lett. 22 (13), 1753–1756, 1995b.

Intriligator, D.S., Wolfe, J.H., Mihalov, J.D. The Pioneer Venus Orbiter plasma analyzer experiment. ISEE Trans. Geosci. Remote Sens. GE-18, 39–43, 1980.

Jian, L., Russell, C.T., Luhmann, J.G., Skoug, R.M. Properties of stream interactions at one AU during 1995–2004. Sol. Phys. 239, 337, 2006a.

Jian, L., Russell, C.T., Luhmann, J.G., Skoug, R.M. Properties of interplanetary coronal mass ejections at one AU during 1995–2004. Sol. Phys. 239, 393, 2006b.

Kivelson, M.G., Russell, C.T. (Eds.). Introduction to Space Physics. Cambridge Univ. Press, Cambridge, UK, p. 588, 1995.

Klein, L.W., Burlaga, L.F. Interplanetary magnetic clouds at 1 AU. J. Geophys. Res. 87, 613, 1982.

Lepping, R.P., Acuna, M.H., Burlaga, L.F., et al. The wind magnetic field investigation. Space Sci. Rev. 71, 207–229, 1995.

Lin, R.P., Anderson, K.A., Ashford, S., et al. A three-dimensional plasma and energetic particle investigation for the Wind spacecraft. Space Sci. Rev. 71, 125–153, 1995.

Liu, Y., Richardson, J.D., Belcher, J.W. A statistical study of the properties of interplanetary coronal mass ejections from 0.3 to 5.4 AU. Planet. Space Sci. 53, 3, 2005.

Liu, Y., Richardson, J.D., Belcher, J.W., Kasper, J.C., Skoug, R.M. Plasma depletion and mirror waves ahead of interplanetary coronal mass ejections. J. Geophys. Res. 111, A09108, 2006.

Marsch, E., Marsden, R., Harrison, R., et al. Solar orbiter mission profile, main goals and present status. Adv. Space Res. 36 (8), 1360–1366, 2005.

McAllister, A.H., Dryer, M., McIntosh, P., Singer, H. A large polar crown coronal mass ejections and a "problem" geomagnetic storm: April 14–23, 1994. J. Geophys. Res. 101, 13497, 1996.

McComas, D.J., Bame, S.J., Barker, P., et al. Solar wind electron proton alpha monitor (SWEPAM) for the Advanced Composition Explorer. Space Sci. Rev. 86, 563–612, 1998.

Neugebauer, M., Goldstein, R. Particle and field signatures of coronal mass ejections in the solar wind, in: Crooker, N., Joselyn, J.A., Feynman, J. (Eds.), Coronal Mass Ejections, Geophys. Monogr. Ser., vol. 99, AGU, Washington, DC, p. 245, 1997.

Ogilvie, K.W., Chornay, D.J., Fritzenreiter, R.J., et al. SWE, a comprehensive plasma instrument for the Wind spacecraft. Space Sci. Rev. 71, 55–77, 1995.

Paularena, K.I., Wang, C., von Steiger, R., Heber, B. An ICME observed by Voyager 2 at 58 AU and by Ulysses at 5 AU. Geophys. Res. Lett. 28, 2753, 2001.

Reisenfeld, D.B., Gosling, J.T., Forsyth, R.J., Riley, P., St. Cyr, O.C. Properties of high-latitude CME-driven disturbances during Ulysses second northern polar passage. Geophys. Res. Lett. 30 (19), 8031, 2003.

Richardson, J.D., Paularena, K.I., Wang, C., Burlaga, L.F. The life of a CME and the development of a MIR: from the Sun to 58 AU. J. Geophys. Res. 107 (A4), 1041, 2002.

Richter, A.K., Luttrell, A.H. Superposed epoch analysis of corotating interaction regions at 0.3 and 1.0 AU: a comparative study. J. Geophys. Res. 91 (A5), 5873, 1986.

Riley, P., Linker, J.A., Mikic, Z., Odstrcil, D., et al. Using an MHD simulation to interpret the global context of coronal mass ejection observed by two spacecraft. J. Geophys. Res. 108 (A7), 1272, 2003.

Russell, C.T., Shinde, A.A. On defining interplanetary coronal mass ejections from fluid parameters. Sol. Phys. 229, 323, 2005.

Russell, C.T., Snare, R.C., Means, J.D., et al. Pioneer Venus fluxgate magnetometer. ISEE Trans. Geosci. Remote Sens. GE-18, 32–36, 1980.

Russell, C.T., Shinde, A.A., Jian, L. A new parameter to define interplanetary coronal mass ejections. Adv. Space Res. 35, 2178, 2005.

Schwenn, R. Large-scale structure of the interplanetary medium, in: Schwenn, R., Marsch, E. (Eds.), Physics of the Inner Heliosphere I, Physics and Chemistry in Space – Space and Solar Physics, vol. 20, Springer-Verlag, pp. 99–181, 1990.

Schwenn, R., Marsch, E. (Eds.), Physics of the Inner Heliosphere I, Physics and Chemistry in Space – Space and Solar Physics, vol. 20, Springer-Verlag, 1990.

Smith, E.J., Wolfe, J.H. Observations of interaction regions and corotating shock between one and five AU: Pioneers 10 and 11. J. Geophys. Res. 3, 137–140, 1976.

Smith, C.W., L'Heureux, J., Ness, N.F., et al. The ACE magnetic field experiment. Space Sci. Rev. 86, 613–632, 1998.

Titov, D.V., Svedhem, H., McCoy, D., et al. Venus Express: scientific goals, instrumentation, and scenario of the mission. Cosmic Res. 44 (4), 334–348, 2006.

Wang, C., Richardson, J.D. Interplanetary coronal mass ejections observed by Voyager 2 between 1 and 30 AU. J. Geophys. Res. 109, A06104, 2004.

Wang, C., Du, D., Richardson, J.D. Characteristics of the interplanetary coronal mass ejections in the heliosphere between 0.3 and 5.4 AU. J. Geophys. Res. 110, A10107, 2005.